This pdf file consists of figures containing photographs, and their captions, scanned from:

STRUCTURE OF THE NORTHERN MARGIN OF THE BITLIS SUTURE ZONE NEAR SIVRICE, SOUTHEASTERN TURKEY

by

Mark R. Hempton

A Dissertation

Submitted to the State University of New York at Albany

in Partial Fulfillment of

the Requirements for the Degree of

Doctor of Philosophy

College of Science and Mathematics

Department of Geological Sciences

1982

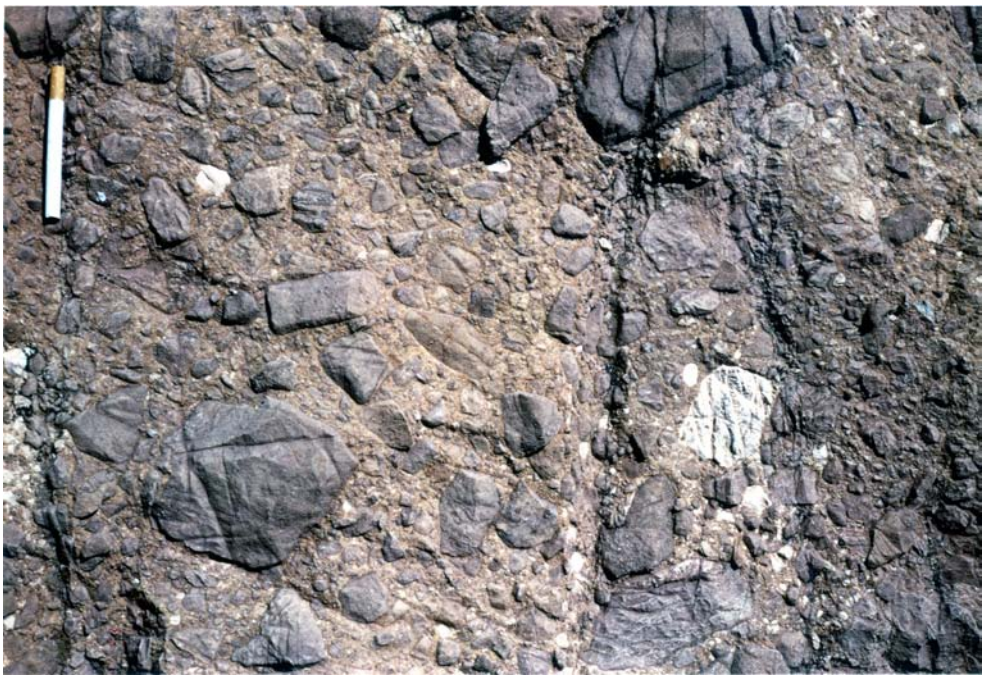

Figure 2.1: Carbonate conglomerate interpreted as a submarine debris flow deposit within Metapelite Unit. Outcrop near Canbey.

Figure 2.2: Transposition fabric in Metapelite Unit near Alaattin. Note disrupted quartz veins and well-developed kink band.

Figure 2.3: Intrafolial folds exhibited by deformed quartz veins in Metapelite Unit. Outcrop near Alaattin.

Figure 2.4: Transposition fabric in outcrop near Alaattin. Note pinch-and-swell nature of some beds and phacoidal shape of segmented boudins.

Figure 2.5: First generation fold in Metapelite Unit. Outcrop near Alaattin.

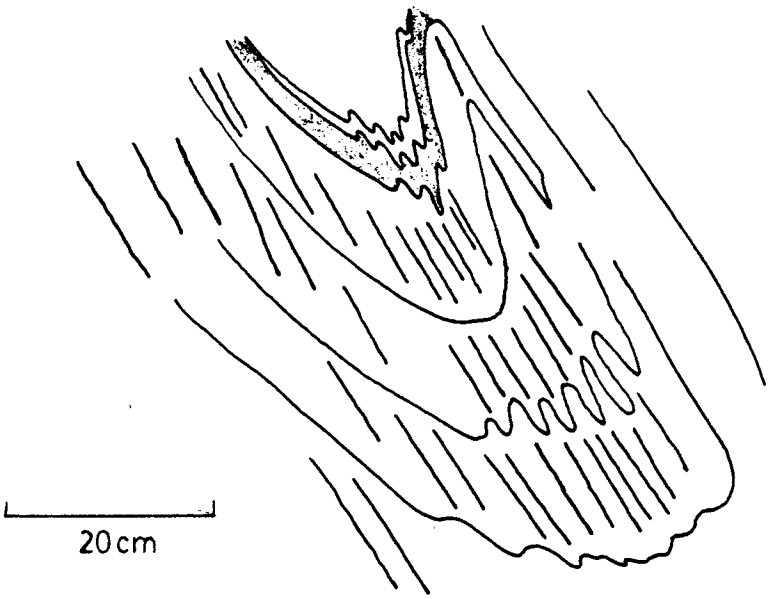

Figure 2.6: First generation fold in Metapelite Unit. Outcrop near Alaattin.

Figure 2.7: Second generation fold in Metapelite Unit. Outcrop near Yukaricanakci.

Figure 2.8: Second generation large concentric fold with small chevron fold in core. Outcrop of Metapelite Unit near Alaattin.

Figure 2.9: Second generation similar fold with weakly-developed second-generation axial planar foliation. Outcrop near Alaattin.

Figure 2.10: Kink band planes in Metapelite Unit. Outcrop near Yukaricanakci.

Figure 2.11: Second generation foliation nearly perpendicular to first-generation foliation in closure of second-generation fold. Outcrop near Alaattin.

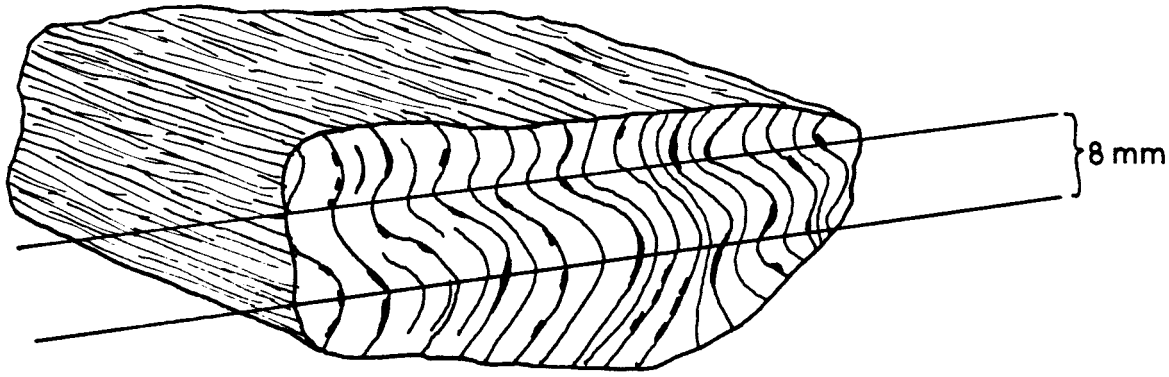

Figure 2.12: Sketch of hand sample of mica schist from the Metapelite Unit. The sample is crenulated on the microscopic and mesoscopic scales. Note 8mm separation of crenulation planes on the mesoscopic scale. Dark blebs are magnetite grains.

Figure 2.13: Very well-developed crenulation cleavage in Metapelite Unit outcrop near Yukaricanakci.

Figure 2.14: Folded first-generation foliation and shear zone in outcrop of Metapelite Unit near Yukaricanakci.

Figure 2.15: Breccia zone in mica schist from Metapelite Unit. Outcrop east of Yukaricanakci.

Figure 2.24: Large exposure of the Recrystallized Limestone Unit near Cefo Mountain exhibiting a great thickness of laterally continuous bedding. Looking SE from a point 2 km NE of Yukaricanakci.

Figure 2.25: Same exposure as in Fig. 24. Looking E from a point 2 km W of Yukaricanakci.

Figure 2.26: Large isoclinal fold in block of the Recrystallized Limestone Unit. Looking S from a point 1 km S of Alaattin.

Figure 2.27: Large isoclinal fold in block of the Recrystallized Limestone Unit. Looking SE from a point 2.5 km W of Samoli.

Figure 2.28: Thinly bedded metaquartzite of the Metapelite Unit. Outcrop 2 km N of Alaattin.

Figure 2.30: Irregular outcrop patterns of Metaquartzite Unit, Recrystallized Limestone Unit, and Metapelite Unit. Looking E from a point 3 km WNW of Alaattin.

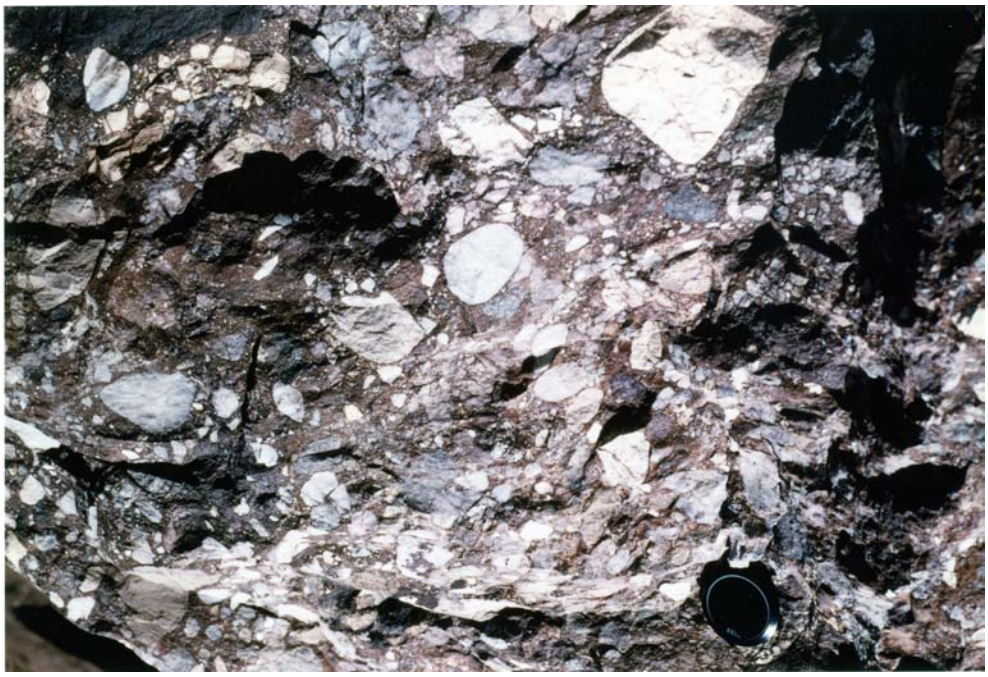

Figure 3.1: Basal conglomerate facies. Outcrop near Keydan.

Figure 3.2: Pelagic limestone facies. Note well-developed cleavage and contorted calcite vein. Outcrop near Keydan.

Figure 3.3: Massive limestone facies. This exposure well-cleaved. Note kink band. Outcrop about 5 km NW of Keydan.

Figure 3.4: Massive limestone facies. Note the many *Nummilites sp.* tests. Note preferred orientation of tests. Outcrop about 4.5 km NW of Keydan.

Figure 3.5: Calcirudite facies. From outcrop near Aluncuk.

Figure 3.6: Tuffaceous mudstone in undifferentiated volcaniclastic facies. Outcrop NE of Kurk.

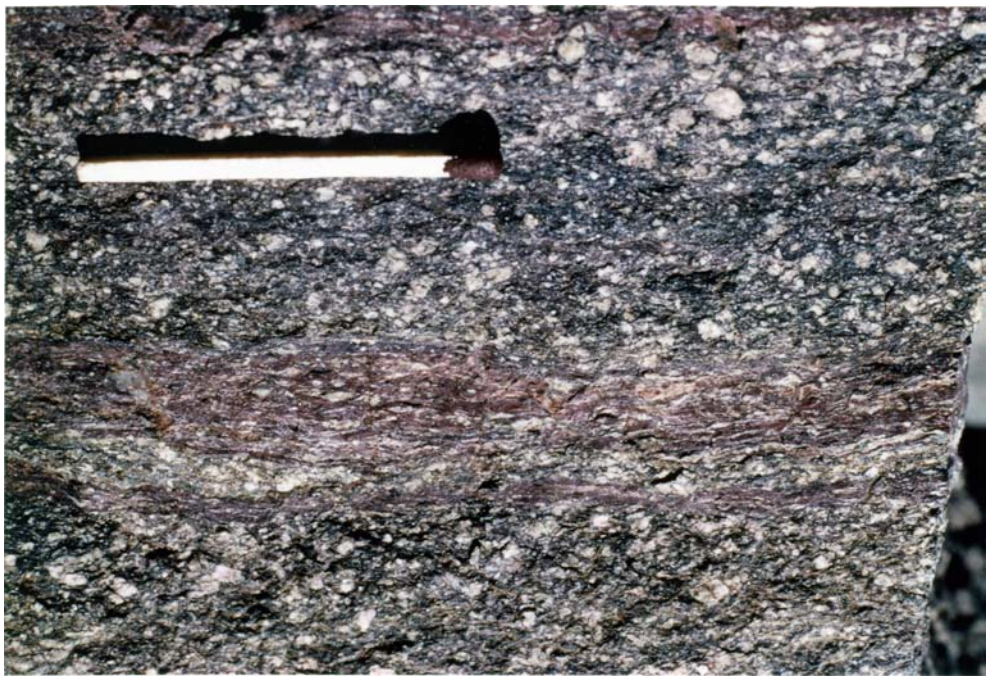

Figure 3.7: Tuffaceous mudstone with many interbeds rich in plagioclase phenocrysts in undifferentiated volcaniclastic facies. Outcrop W of Keydan.

Figure 3.8: Tuffaceous conglomerate in undifferentiated volcaniclastic facies. Outcrop near Gomolar.

Figure 3.9: Tuffaceous conglomerate in undifferentiated volcaniclastic facies. From outcrop near Karik.

Figure 3.10: Tuffaceous conglomerate in undifferentiated volcaniclastic facies. From outcrop near Sogukpinar.

Figure 3.12: Deformed undifferentiated volcaniclastic facies. In this outcrop N of Keydan the matrix is defined by tuffaceous mudstone. Note how stretched individual boudins appear..

Figure 3.13: Deformed undifferentiated volcaniclastic facies with thin, stretched, pinched, and folded interbeds. Note thin calcite veins perpendicular to fabric.

Figure 3.14: Well-cleaved undifferentiated volcaniclastic facies with very elongate boudins.

Figure 3.15: Chevron fold in well-cleaved undifferentiated volcaniclastic facies. North is to the left.

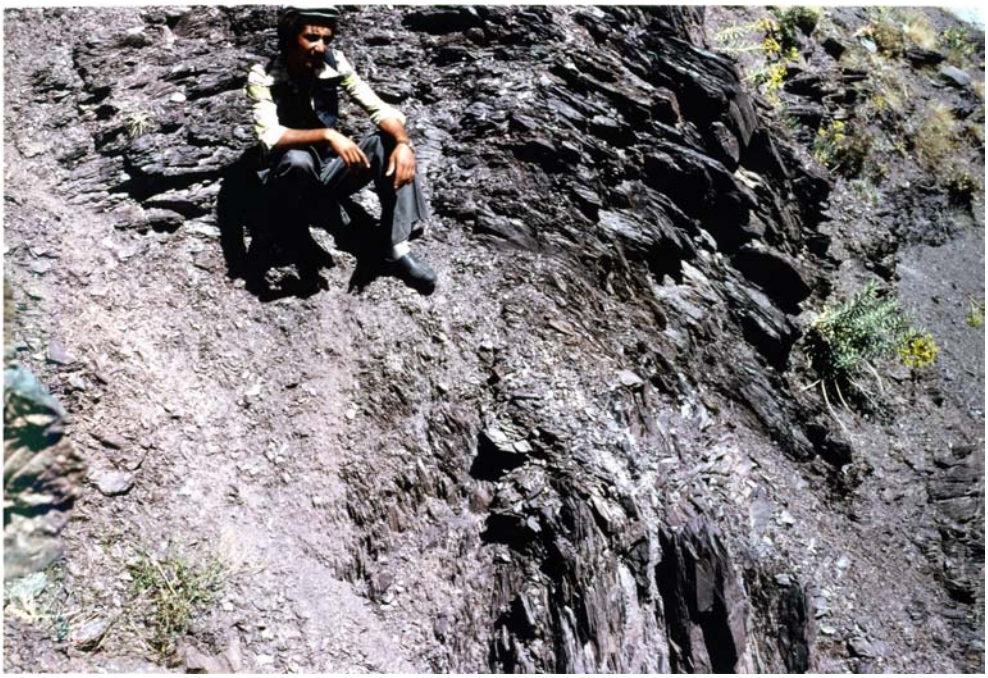

Figure 3.16: Cylindrical fold in well-cleaved undifferentiated volcaniclastic facies. Outcrop E of Karik.

Figure 4.1: Isotropic metagabbro with gabbro pegmatites.

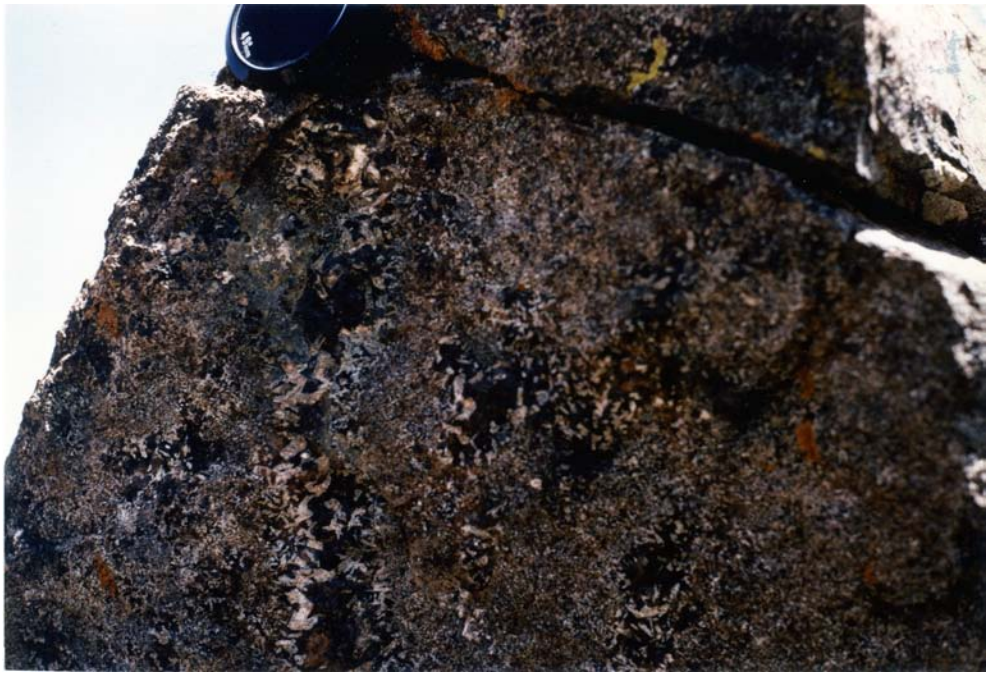

Figure 4.2: Metagabbro exhibiting great variation in grain size. Note very large grains concentrated in clusters.

Figure 4.3: Layered metagabbro. Note grading in bed at left.

Figure 4.5: Apparent channel within layered metagabbro.

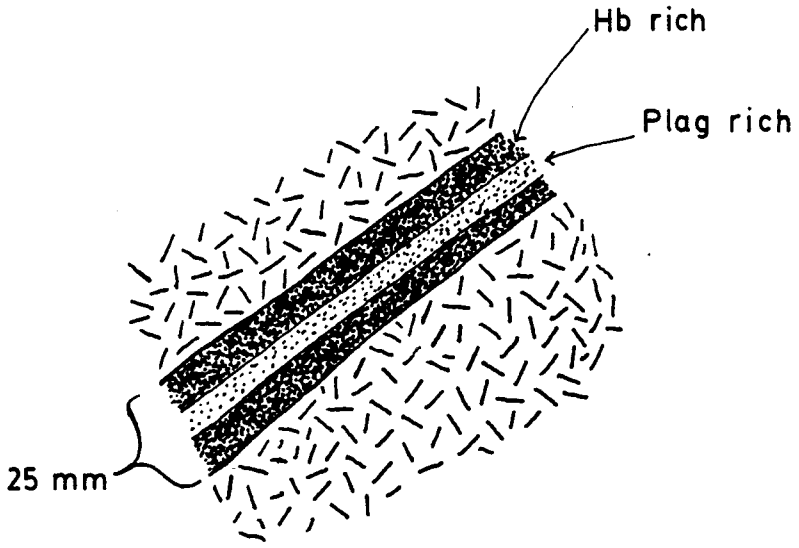

Figure 4.7: Thin zoned diabase dike in metagabbro.

Figure 4.8: Thick diabase dike within metagabbro.

Figure 4.9: Metagabbro intrusion in metagabbro.

Figure 4.10: Thick, laterally continuous silicic dike in metagabbro.

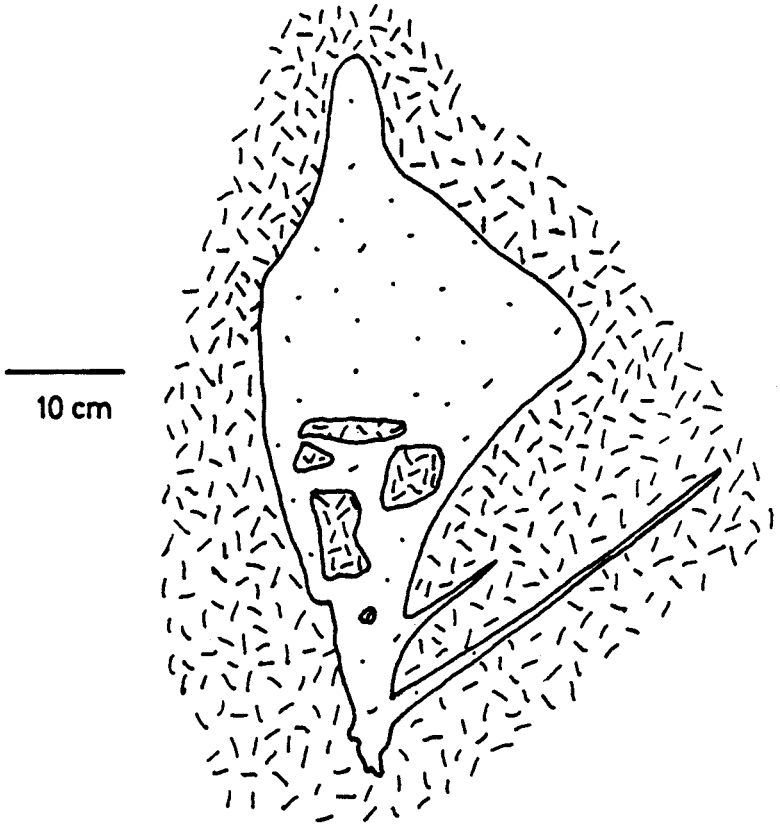

Figure 4.11: Silicic intrusion in metagabbro.

Figure 4.12: Silicic dikelet with irregular margins and thin extensions as fracture fill in metagabbro.

Figure 4.14: Thin fine-grained diabase dike in porphyritic diabase.

Figure 4.15: Thin fine-grained diabase dike in metagabbro. Note chill margins.

Figure 4.16: Thick fine-grained diabase dike in diabase.

Figure 4.17: Thin medium-grained diabase dike in microgabbro.

Figure 4.18: Diabase dike with gradational change in texture from fine-grained at the margin to coarse-grained in the center.

Figure 4.19: Diabase dike with chill margins grading toward coarse-grained center.

Figure 4.20: Dike contact between fine-grained diabase with chill margin and porphyritic diabase.

Figure 4.21: Thin diabase dike with central band rich in plagioclase phenocrysts.

Figure 4.22: Diabase dike with subparallel plagioclase-rich and plagioclase-poor bands.

Figure 4.23: Anastomosing diabase dikes among screens of metagabbro.

Figure 4.24: Thin diabase dike that makes sharp turn.

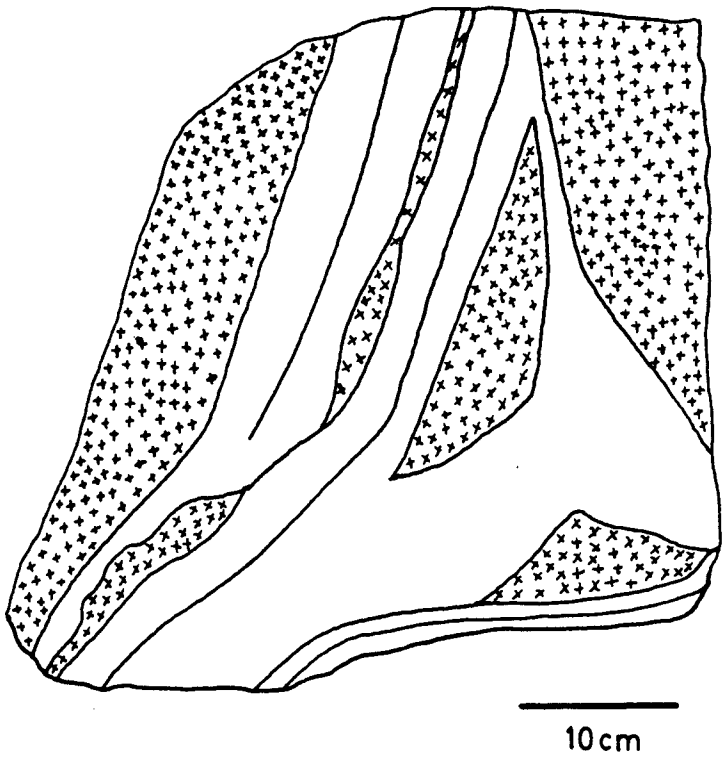

Figure 4.25: Anastomosing diabase dikes that isolate screens of metagabbro.

Figure 4.26: Thin diabase dike that cuts layered metagabbro.

Figure 4.28: Thin diorite dike in diabase.

Figure 4.29: Injection breccia – diorite matrix with diabase clasts.

Figure 4.30: Diabase dike that cuts diorite.

Figure 4.31: Typical outcrop of pillow basalt.

Figure 4.33: Breccia horizon within Basalt Unit.

Figure 4.29: Andesite dike cutting Basalt Unit.

Figure 4.35: Layering in metagabbro stock which outcrops in Basalt Unit. White layer is altered plagioclase. Dark layer is rich in hornblende.

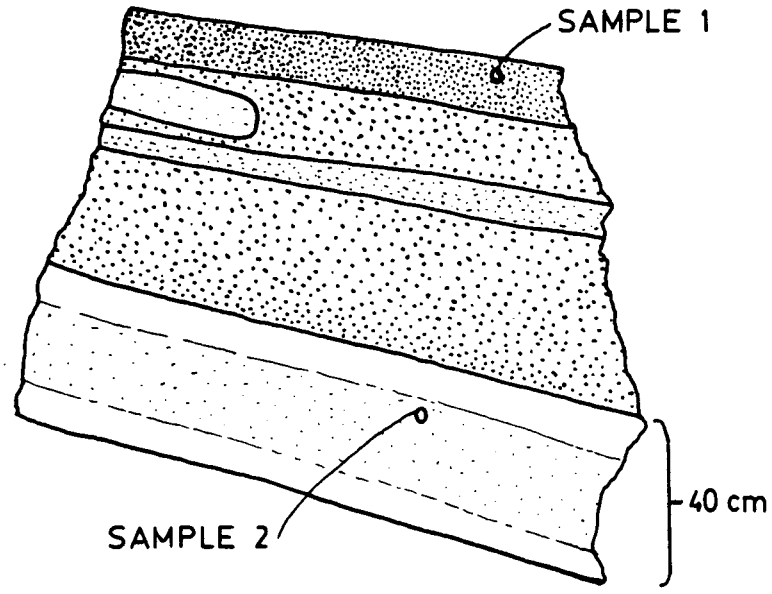

Figure 4.36: Layering in diorite stock which outcrops in Basalt Unit. Whiter layers are richer in plagioclase and quartz. Darker layers (stippled) are richer in hornblende.

Figure 4.37: Silicic dike cutting basalt in Basalt Unit.

Figure 4.38: Quartz vein cutting basalt in Basalt Unit. Note offset.

Figure 4.39: Porphyritic andesite volcanic flow in Andesite Unit.

Figure 4.40: Contact between andesite volcanic flows with different proportions of plagioclase phenocrysts (in Andesite Unit).

Figure 4.41: Thin section of porphyritic andesite from Andesite Unit.

Figure 4.42: Andesitic pyroclastics outcropping in large exposure south of Lake Hazar.

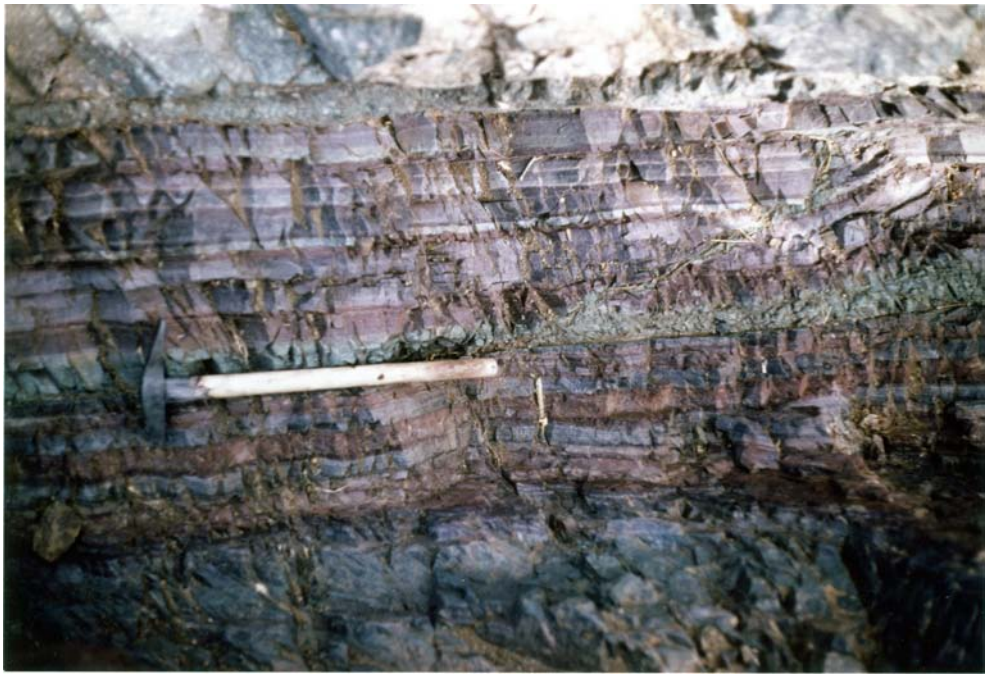

Figure 4.43: Thinly interbedded andesitic volcaniclastic fall deposits.

Figure 5.1: Fault block and scarp composed of Simaki Formation rocks in center and right of photograph. SE shore of Lake Hazar near Sivrice. Looking SE.

Figure 5.2: Interbedded fine-grained sandstone and mudstone (light beds) and fine-grained limestone beds (dark beds) of Simaki Formation. Near middle of section.

Figure 5.4: Like Figure 5.2 except for greater proportion and thickness of dark grey limestone interbeds. Near top of section of Simaki Formation.

Figure 5.8: Small serpentine sliver in thrust fault zone near Migirgan. About 25 by 5 m.

Figure 5.9: Spheroidal weathering of serpentine sliver in southwestern thrust fault zone between Migirgan and Kurk.

Figure 6.1: A thin thrust sliver of purple Maden Complex lying between Elazig Complex above and Pütürge Complex below. Looking northeast. Photo taken from a point 1km southeast of Alaattin.

Figure 6.2: Metaquartzite breccia. Outcrop located about 2km south of Karik.

Figure 6.3: Polished stream boulder of metaquartzite breccia. About 2 km SW of Alaattin.

Figure 6.4: Nearly horizontal thrust contact between orange-weathering Elazig Complex above and purple-weathering Maden Complex below. The contact is about two thirds of the way up the ridge between the train and the top. Looking west from the Elazig-Diyarbakir road.

Figure 6.5: Thrust contact between orange-weathering Elazig Complex to the left and purple-weathering Maden Complex to the right. Looking north from Aluncuk.

Figure 6.6: Thrust contact between orange-weathering Elazig Complex above and purple-weathering Maden Complex below. Looking west. Photo taken from a point about 2.5 km north of Kurk.

Figure 6.7: Thrust contact between orange-weathering Elazig Complex above and purple-weathering Maden Complex below. Photo taken from along Kurk road about 3 km east of Kurk.

Figure 6.8: Closer view of thrust contact from Figure 6.7. Note fault plane asperities and gouge zone.

Figure 8.1: Southern boundary of Megabreccia Zone marked by narrow, deep fault-line valley. Looking SW from a point 500 m west of Kazkiran.

Figure 8.2: Megabreccia derived from the Maden Complex. Looking NE from a point 1 km east of Uslu. Note 'layers' of megabreccia.

Figure 8.3: Megabreccia derived from the Maden Complex. Note large white patch of breccia enveloped by purple breccia. Looking E from a point 1 km W of Isolar.

Figure 8.4: Block in megabreccia derived from metamorphics. Looking E from a point 1 km NW of Gedik.

Figure 8.6: Horizontal contact between overlying breccia which is relatively more coherent, and underlying fine-grained breccia. Looking W from a point 2 km NE of Karik.

Figure 8.7: Gravel offset about 3 m along fault with reverse displacement. Approximately 300 m W of Kurk. Looking S.

Figure 8.12: South wall of the East Anatolian Fault zone. Looking S from a point 1 km NE of Kurk.